ICANS XIX,
19th meeting on Collaboration of Advanced Neutron Sources
March 8 – 12, 2010
Grindelwald, Switzerland

NEUTRON OPTICS SIMULATIONS FOR THE UCN SOURCE AND NEDM PROJECTS AT PSI

Z. Chowdhuri, G. Zsigmond
on behalf of the UCN Project Team[1] and nEDM Collaboration[2]
Paul Scherrer Institut, Villigen, Switzerland

ABSTRACT

A superthermal ultracold neutron (UCN) source is in the final stage of construction at the Paul Scherrer Institut (PSI). It is designed to deliver about two orders of magnitude larger UCN density than the currently strongest UCN source PF2 at ILL. The flagship experiment performed by an international collaboration at the PSI UCN source targets the measurement of the neutron electric dipole moment (nEDM) using the Ramsey method of separated oscillatory fields.

Both projects are strongly supported by Monte Carlo simulations. One scope is to optimize the UCN optics as a function of geometry and wall coating properties in order to achieve maximal UCN density in the experiment. Another scope is the support of systematics calculations in the nEDM measurement since, in a Monte Carlo model, different systematic contributions can be separated, thus helping the estimations of these for the real apparatus.

The model of the PSI source and the connected UCN optics system of the nEDM apparatus, implemented in the MCUCN ray tracing code, and recent results will be presented.

1. Introduction

The UCN source at the Paul Scherrer Institut, Switzerland, will use a pulsed spallation source and solid deuterium for the generation of ultracold neutrons [1]. The working principle is described in detail in Ref. [2]. Commissioning started in fall 2009. An international collaboration [3] is simultaneously setting up an experiment to search for the electric dipole moment of the neutron.

One scope of the Monte Carlo (MC) simulations is the optimization of UCN optics to achieve maximal density in the nEDM experimental chamber. Another goal is to support in a later stage systematics calculations. In a simulation model different systematic contributions can be switched on/off thus helping in the estimations of these for the real apparatus.

At present, a full Monte Carlo model is available for the PSI source and the UCN optics of the nEDM apparatus. The UCN source and nEDM experiment are part of the same simulation model since UCN travel multiple times through the whole system during the filling phase of the precession chamber. In this paper we briefly present simulation results obtained recently.

2. The simulation code MCUCN

Simulations were performed using the C++ code MCUCN [4]. This is the second 3D ray tracing code developed in the UCN Physics Group at PSI besides GEANT4UCN [5]. It is used at present in UCN projects at PSI and TU-Munich.

---

[1] ucn.web.psi.ch/people.htm; [2] nedm.web.psi.ch

In the present MCUCN simulation model we have included all important geometry details of the UCN source, the guiding system and the UCN-related nEDM experiment parts. We define the walls by second order surfaces with boundaries including time dependence (switching on-off shutters). The main coating parameters for the MC simulations are defined as in Ref. [6]:
(i) material optical potential, a.k.a. Fermi potential, V_{Fermi} (typically 230 neV);
(ii) parameter for wall losses, η (typically 3×10^{-4}) due to absorption and up-scattering – it is defined as a ratio of the real and imaginary part of the Fermi potential; based on this definition, the loss probability per bounce becomes an energy and direction dependent function;
(iii) diffuse scattering probability (typically 2%) following the Lambert (cosine distribution) model; other diffusivity models as Gaussian blurring around the specular direction, a micro-roughness model based on wave interference [7] have also been implemented;
(iv) spin flip probability per bounce on the walls;
(v) gravity as an important force for UCN (generates 1 neV kinetic energy difference per cm);
(vi) implementation of spin precession in general weak magnetic fields (no influence on the trajectory) is in progress.

MCUCN calls no external libraries and thus it is very flexible in grid computing. No parallelization is implemented yet, however, jobs with different random generator seeds can be distributed to a large number of CPUs and the output data are collected easily by shell scripts.

It is very efficient to apply two codes in parallel since these can thus be benchmarked against each other and against the experiments. Programming failures and simulation artifacts can be identified and fixed more quickly. Inter-comparisons of MCUCN and Geant4UCN performed up to now gave good agreement.

3. MC model of the PSI UCN source and nEDM apparatus

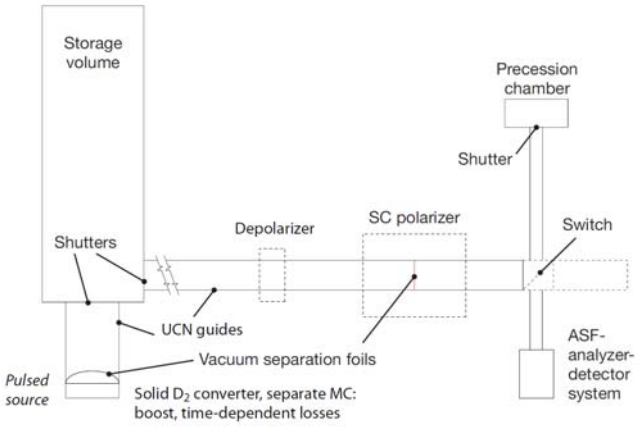

Fig. 1: Main building blocks of the MC model (see text). Dimensions not to scale.

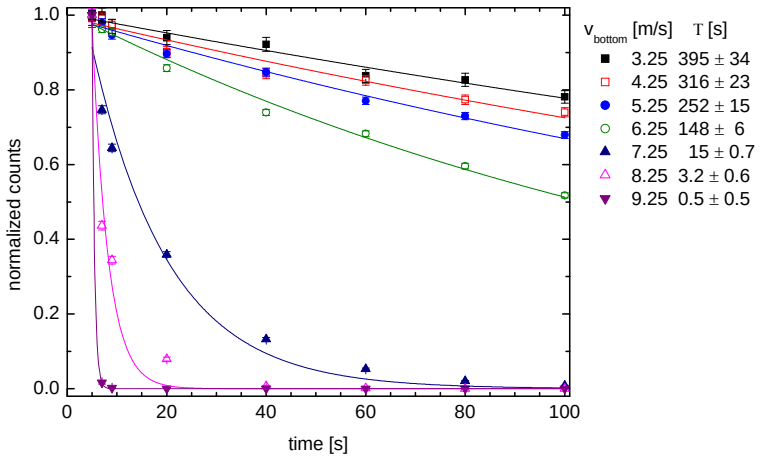

Fig. 2: Storage curves of UCN in the source storage volume with different velocities at the bottom

The main elements of the simulation model discussed here are depicted in Fig. 1. On the left hand side one can identify the UCN source components. Details on the source setup can be read in Ref. [2].

Calculations of the storage curves of UCN in the source storage volume with different bottom velocities are illustrated in Fig. 2. Two bunches of decay curves separated from each other indicate that in one case the bottom velocity is below the limit velocity of the coating determined by the Fermi potential of the wall (time constants T between 150-400s) and in the other case it is above this limit. This means that the overall spectrum will be cleaned from neutrons above the maximal UCN energy (i.e. approx. Fermi potential) on a scale of 20-40 s.

On the right hand side of Fig. 1, the UCN optics components of the nEDM experiment, which is connected to the source by cylindrical NiMo coated guides, are also plotted. The source and the nEDM apparatus are one system in the filling phase: UCNs travel multiple times between the experiment chamber and the storage volume of the source. The components necessary for an effective polarization – 'Depolarizer' and 'SC (superconducting) polarizer' – and corresponding simulations of the filling efficieny of the experimental storage chamber ('Precession chamber') were presented earlier [4, 8].

Since then we have concentrated on the adiabatic spin flipper(ASF)-analyzer-detector system which is necessary to detect both spin components emerging from the experiment, i.e. to perform a complete polarization analysis. We placed particular emphasis on different geometries for the simultaneous analysis of the spin up and down neutrons.

First we show as short examples three other representative MC results for the nEDM experiment, providing information on the filling and storage time constants as a function of UCN energy in the chamber (Figs. 3a,b). The data are illustrated by snapshots of the UCN density at different time moments. The spectrum of the PSI UCN source, and consequently that in the chamber, will define the offset between the center of gravity of UCN and the center of the chamber (Fig. 4). Since faster UCN are lost at higher rates, this offset increases with storage time. This will be an important input for systematics calculations of the nEDM [9].

Several analyzer-detector geometry options (see location on the right side of Fig. 1) were studied for a simultaneous analysis of the spin up and down components. The idea is to have two readout arms, each arm with a polarization analyzing system and detector. They would be configured so that the two spin states would be separately but simultaneously counted. The two-arm method would have another advantage in that it would be insensitive to intensity variations in the source. In contrast to reactor-based UCN sources, accelerator-based sources are prone to intensity variations and proper normalization is crucial. An additional spin flipper in each arm allows the detected polarization component to be switched. A possible realization is sketched in Fig. 5(i). The neutrons enter from the top via a short guide coming from the switch. Immediately afterwards, the guide separates into two parts which form a double detector chamber separated by a thin, coated wall. This wall could be a thin sheet which is necessary to hold and separate the two adiabatic spin flipper coils (ASF). The polarization analyzer foil in front of the detector also needs a strong permanent magnetic field and this poses an additional space problem to be solved. A large volume of the detector chamber in comparison to the entering guide favors UCN to stay close to the detectors if they bounce back due to having the wrong spin state.

In the following we summarize the results for the different geometry options: (1) compact geometry (simultaneous analysis), (2) Y-shaped geometry (simultaneous analysis), and (3) single-detector geometry for sequential analysis. We will call “spin up” the state when the spin is parallel to the analyzer field and vice versa. Spin flips on the walls were not considered at this stage.

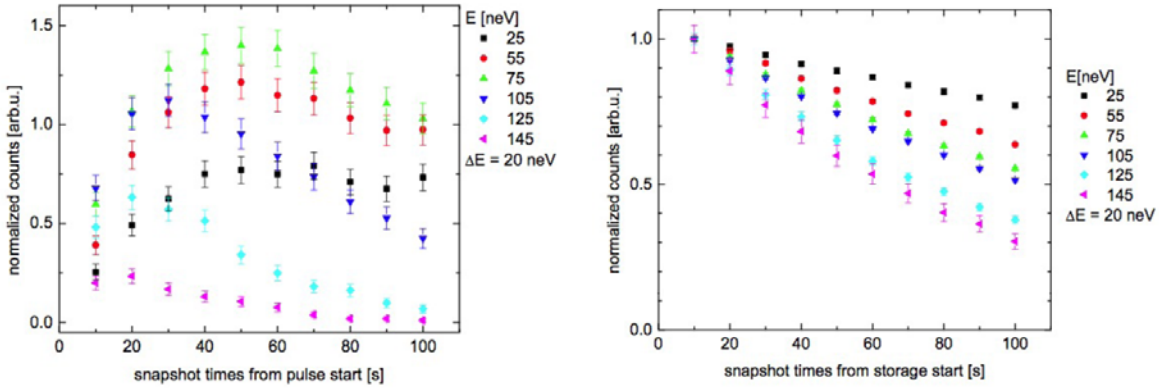

Fig. 3: (a) UCN in the chamber vs filling time as a function of kinetic energy; (b) UCN in the chamber vs storage time as a function of kinetic energy.

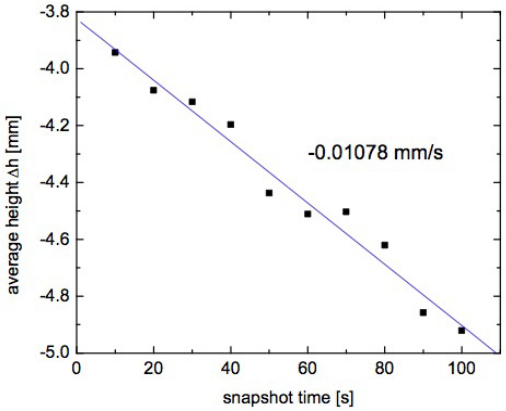

Fig. 4: Center of gravity offset between UCN and mercury for the PSI source spectrum in the chamber vs storage time.

(1) Compact geometry – The effect on the neutron transport of materials with different Fermi potentials, of the quality of the surfaces and also of the geometry of the system has been studied in order to optimize the fraction of the stored UCN that arrive at the detection system.
Geometry of the detector assembly: We want to minimize the loss of UCN as they travel from the precession chamber to the detector and we want to maximize the accurate simultaneous detection of the two neutron spin states. Fig. 5 depicts three possible congurations under consideration. In the first two cases the detectors for the two spin states are arranged next to each other (side-by-side configuration) while in the third they face each other [10]. A set of simulations has been completed for configuration (i); work is in progress for the other two. The variation of the number of neutrons at the detector with changes in the height of the upper detector guide (shaded region) is shown in Fig. 6(a).

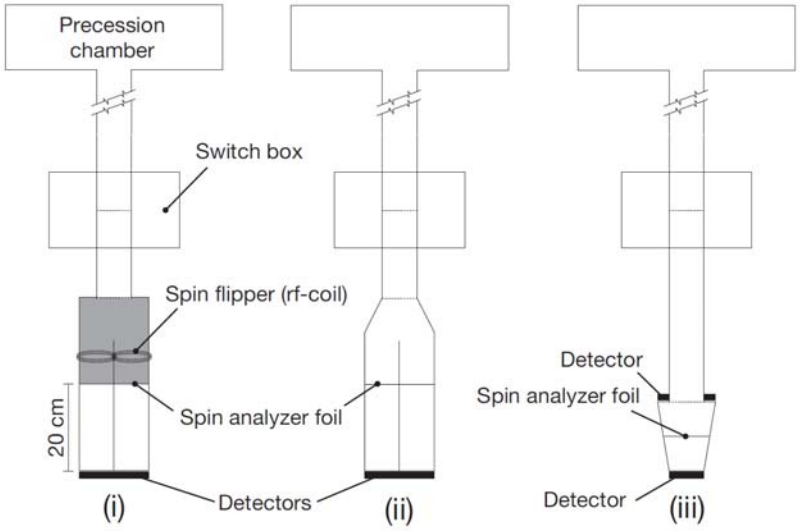

Fig. 5: Different detector configurations that are being considered for the simultaneous detection of both spin state neutrons. The heavy line segments represent the neutron detection elements.

Surface quality and Fermi potential – Four different values of surface roughness and two different values of the Fermi potentials for the wall materials were compared to study how the transport of neutrons from the chamber to the detector depends on these. The results for the case of configuration (i) in Fig. 5 are shown in Fig. 6(b). As the diffuse parameter of the surface becomes worse, it becomes more important to use a material with higher Fermi potential.

(2) Y-geometry The Y-geometry (see also Ref. [11]) is shown in the left panel of Fig. 7. The vertical guide section just below the guide switch branches out to two analyzer arms. On one arm an ASF is added. On the right side of the figure the extracted fractions of the stored UCN are compared for different angles of the arms. The efficiency would be about 75% for a diffuse reflection probability of 2%.

(3) Single-detector geometry for sequential analysis – The case of sequential analysis, which is well known from the nEDM apparatus at ILL [9], was also computed for comparison. The sequence consists of an 8 s measurement for the spin down (SF off), 20 s for spin up (SF on) and 12 s for the spin down (SF off). The spin down UCN see a 90 neV polarizer foil potential and the up spin UCN see 330 neV. Since one spin component is

differently stored as the other, the efficiency is not automatically symmetric for the two spin states. However, by adjusting the detection times sequence, the efficiency can be made symmetric.

For a fair comparison, as treated below, the geometry of both the sequential and compact cases was set similar to the Y-geometry: the polarizer foil was about 65 cm below the beam axis; the detector window was at 15 cm below the polarizer foil; and diffuse fractions of 1, 2 and 4% (guide coatings) were considered by keeping the other surface parameters the same.

We compare the detection time profiles to the profiles of the 'Y' (30° angle between the arms) and compact geometries used for the simultaneous analysis as plotted in Fig. 5. The energy dependent wall losses were determined to be $\eta = 3\times10^{-4}$ as in the previous cases. The results are summarized in Tab. 1.

We conclude from these simulations that simultaneous analysis is the most advantageous given the higher effciency, inherently symmetric count rates, and shorter detection times.

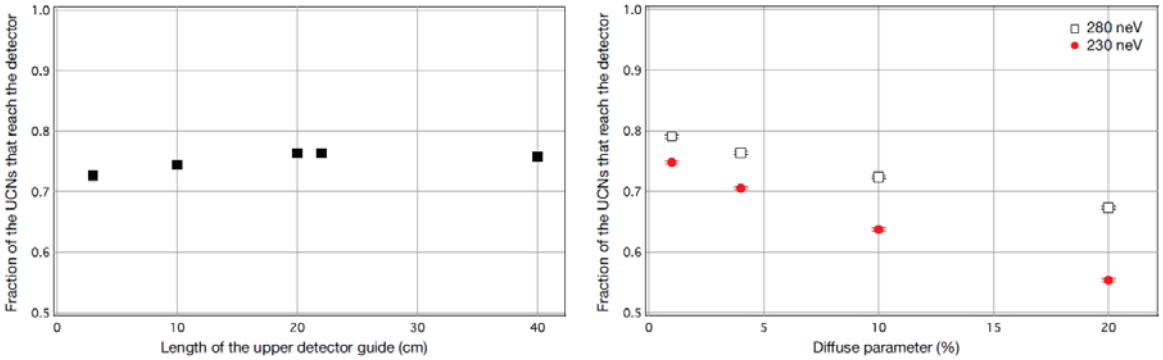

Fig. 6: Compact geometry results – (a) The nominal length of the upper guide is taken to be 20 cm where it appears to be well optimized; (b) The effect of surface type and quality on the fraction of UCNs at the detector. As the diffuse parameter increases, the importance of having a high Fermi potential increases.

	down			up		
Analysis Diffuse:	0.01	0.02	0.04	0.01	0.02	0.04
Sequential	75	72	68	65	62	57
Simultaneous - Y geom	77	74	70	77	74	70
Simultaneous - compact geom	79	76	73	79	76	73

Table 1: Comparison of detection efficiencies (in %) of the up and down spin components for the sequential and simultaneous ('Y' or compact geometries) analysis as function of the fraction of diffuse reflections.

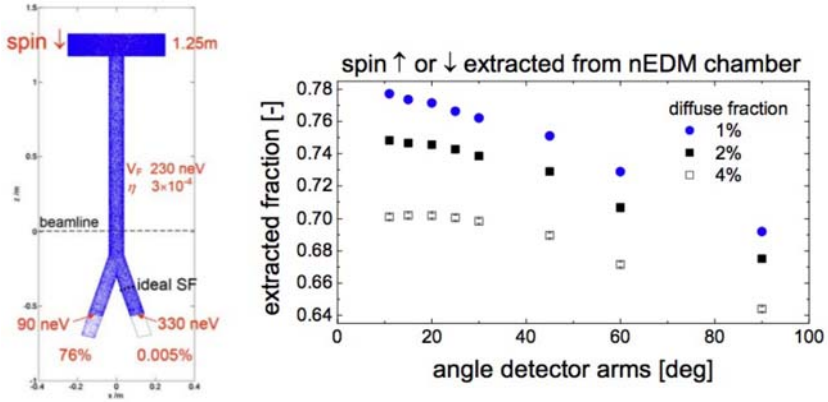

Fig. 7: Y-shaped system geometry and estimates for the efficiency as function of angle between detector arms.

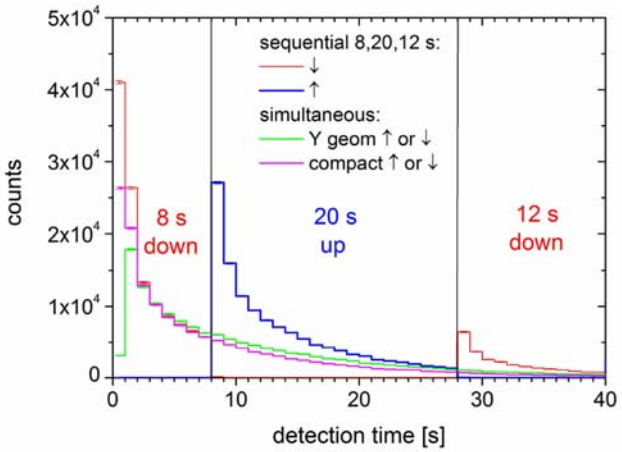

Fig. 8: Detection time profiles of the sequential analysis compared to the profiles of the Y and compact geometries for 2% diffuse fraction (see text).

4. Conclusions and outlook

We have illustrated in this contribution that MC simulations could be effectively applied to extract UCN source parameters like velocity dependent storage time constants as well as to identify the most optimal option for the analyzer-polarizer-detector geometry. Further study will target, amongst others, detailed figure of merit calculations for the nEDM polarization analysis, including depolarization effects. The final goal is to simulate the full polarization analysis sequence of the nEDM measurement to study systematic effects with both codes MCUCN and GEANT4UCN.
The two simulation codes are available for similar projects via Ref. [12].

References

[1] Website of the PSI UCN source: ucn.web.psi.ch
[2] B. Blau, W. Wagner, Status of the Ultracold Neutron Source at PSI (these proceedings)
[3] Website of the nEDM collaboration based at PSI: nedm.web.psi.ch
[4] NOP09 proceedings paper (in print)
[5] F. Atchison et al., Nucl. Instr. and Meth. A552 (2005) 513
[6] R. Golub, D. Richardson, and S. K. Lamoreaux, 1991, Ultracold Neutrons (Adam Hilger, Bristol)
[7] A. Steyerl, Z. Physik 254 (1972) 196
[8] P. Geltenbort et al, Nucl. Instr. and Meth. A608 (2009) 132
[9] C. A. Baker et al., Phys. Rev. Lett. 97 (2006) 131801
[10] M. S. Lasakov, Nucl. Instr. and Meth. A545 (2005) 301
[11] M. G. Rogel, PhD Thesis, 2009, University of Caen
[12] Website of UCN MC: ucn.web.psi.ch/mc